



Fractional Order ANFIS Sliding Mode Controller for Two-Time Scale Dynamics in PWR

Arshad Habib Malik^{1*}, Feroza Arshad², and Aftab Ahmad Memon³

¹Faculty of Engineering, Information and Technology, Sindh Institute of Management and Technology, Karachi, Pakistan

²Department of Information System Division, Karachi Nuclear Power Generating Station, Pakistan Atomic Energy Commission, Karachi, Pakistan

³Faculty of Electrical, Electronic and Computer Engineering, Mehran University of Engineering and Technology, Jamshoro, Sindh, Pakistan

Abstract: In this research work, a novel model of Pressurized Water Reactor (PWR) dynamics is developed with special emphasis on nuclear fuel burn-up or fuel depletion dynamics. PWR dynamics is identified and decomposed into fast and slow dynamic modes for the first time in this research work. The stiff two-time scale reactor dynamics problem is addressed, and a new sophisticated fractional order two-time scale sliding mode controller is designed. The PWR dynamics is uncertain due to three distinct operating conditions of nuclear reactor core as Beginning of Core (BOC), Middle of Core (MOC) and End of Core (EOC) synthesizing a variable structure model. The model uncertainties are estimated using Adaptive Neuro-Fuzzy Inference System (ANFIS) while different reactivity components are addressed as active disturbance or measurement noise. The novel robust control design problem is a big challenge in this research. The proposed controller is designed, tested and validated against benchmark data and found excellent in performance.

Keywords: Fractional Order Control, ANFIS, Two-Time-scale, Sliding Mode Control, Burn-up, PWR.

1. INTRODUCTION

Currently, control methods for PWRs are incapable of handling the dynamic uncertainties due to fuel burn-up and thermal reactivity variation under various conditions. The goal of this study is to design a flexible control system that takes into consideration these incalculable factors in order to keep a reactor in check in terms of steady and efficient operation. The reactor core model is developed through a lumped parameter thermo-neutronic coupled reactor dynamics. The dynamic behavior of the fuel burn-up is incorporated. Two new external reactivity controllers are designed; one with only thermal reactivity feedback and other with reactivity feedback due to fuel burn-up and poisons. A detailed literature review is conducted to address the modeling and controller design

techniques in general and PWR in specific. Various linear, nonlinear, integer order, fractional order, neural, fuzzy, neuro-fuzzy and hybrid methods are studied, and their pros and cons are established. System dynamics with certainty and uncertainty are also studied so that a suitable and most accurate method could be established for PWR dynamics and control. An adaptive fractional order PID controller is designed for liquid level fine control system by Reddy *et al.* [1]. Similar study is also conducted for nuclear reactor point reactor kinetic model by Safarzadeh *et al.* [2]. A higher order observer is synthesized for PWR dynamics with thermal feedback by Ahmed *et al.* [3]. A point reactor kinetics-based model is developed for same PWR which is under consideration with thermal feedback and a nonlinear sliding mode observer is attempted by Hussain *et al.* [4]. This research provides a basis

for current research work to extend with more detailed dynamics and extended controller design. A fractional order adaptive neuro-fuzzy inference system (ANFIS) controller is attempted for droop control of wind turbine by Asgharpour-Alamdari [5] which is an intelligent control on fractional scale. A hybrid controller based on adaptive fuzzy fractional order sliding mode control technique is established for a dynamic system by Ullah *et al.* [6]. This is a class of uncertain system dynamics. Another hybrid controller based on adaptive fuzzy fractional order sliding mode control technique is formulated for micro gyroscope system by Liang and Fei [7]. This research uses a backstepping technique for nonlinear controller design. Similarly, a hybrid controller based on adaptive neural fractional order sliding mode control technique is established for micro electro-mechanical system (MEMS) by Fei and Lu [8]. This research uses a backstepping technique for nonlinear controller design. Another hybrid controller based on adaptive neural fractional order sliding mode control technique is addressed for ultrasonic motor by Chen *et al.* [9]. This design incorporates neural network compensation technique. A H_{∞} sliding mode controller is a different control design configuration adopted for 2500 MW_{th} PWR type nuclear reactor by Kirgni *et al.* [10]. Kalman filters, LQG and fractional order sliding mode controllers are designed for uncertain single input single output systems such as PWR reactor power control, reactor coolant temperature control, pressurizer level control, steam generator pressure control and turbine speed control by Surjagade *et al.* [11]. This is a comprehensive model-based controllers' design work and provides a strong basis to extend such fractional order nonlinear SMC for other systems with unique dynamics. A fractional order sliding mode controller is adopted for an uncertain nonlinear system by Zhang *et al.* [12] which is designed based on LQR technique. Research is further explored for ANFIS based sliding mode control for coupled tanks system by Boubakir *et al.* [13] which is a hybrid control design scheme comprising of intelligent control and nonlinear sliding mode control. A similar ANFIS based SMC is synthesized using Harmony Search Optimization technique by George and Mani [14]. An investigation is conducted for uncertain chaotic systems using ANFIS based sliding mode controller by Akbari *et al.* [15]. An adaptive neuro-fuzzy fractional order terminal sliding model controller is designed for micro gyroscope system

using backstepping technique by Fei and Liang [16]. A multi-loop adaptive neuro-fuzzy fractional order sliding model controller is attempted for micro gyroscope system by Fang *et al.* [17]. In this research, a multivariable ANFIS based FO SMC is considered which provides a strong basis that new controller could be adopted with some new framework of model.

In this research work, a new model is proposed for reactor dynamics of PWR type nuclear power plant in two-time-scale framework with an addition of burn-up or fuel depletion modeling for the first time. A novel hybrid Fractional Order Adaptive Neuro-Fuzzy Inference System (ANFIS) based Two-Time-Scale Sliding Mode Controller (FO-ANFIS-TTS-SMC) is designed for proposed model of medium scale 300 MWe PWR nuclear power plant under BOC, MOC and EOC as variable nonlinear complex operating conditions of reactor core which formulates a unique complex challenging engineering and computing problem. The aim of this research work is to design and analyze the external reactivity controller for the control of reactor core thermal power, fuel and coolant temperatures of 998 MW_{th} Pressurized Water Reactor type Nuclear Power Plant.

2. MATERIALS AND METHODS

2.1. Modeling of PWR Dynamics

A 300 MWe PWR type nuclear power plant is considered for proposed design, simulation and analysis purposes. Various parameters/symbols and variables used hereafter in PWR dynamics modeling are adopted from Hussain *et al.* [4] while rest of parameters/symbols used in extended modeling and novel controller design are defined in Table 1. The PWR dynamic model is developed in time domain and space dependent effects are not considered throughout the modeling. The sampling interval is 0.001 second and the scale separation factor is 0.12. The exact values of the initial model parameters such as fuel temperature, coolant temperature, reactivity and burn-up are adopted from research work conducted for same PWR [4]. The dynamics of PWR reactor power is modeled as [4]:

$$\frac{dn_r(t)}{dt} = f_n((\rho_{net}, \beta_{eff}, \Lambda, n_r, C_r), t) \quad (1)$$

Table 1. Symbols/parameters of model and controllers.

Parameters	Definitions
N	Number Density of Radio Nuclide
L	U-235, U-238, Pu-239, Pu-240, Pu-241
P	Poison Nuclide
K_∞	Infinite Multiplication Factor
γ	Yield Fraction
φ	Premise Variable
r	Fuzzy Sets
R	Fuzzy Rules
U	Control Input
X	State Vector
Y	Output Variable
δ	Uncertainty Nonlinear Function
D	Disturbance Nonlinear Function
I	1, 2, ..., n_1
J	1, 2, ..., n_2
μ	Scale Separation Factor
M	Identity Matrix
ψ	Normalized Membership Function
G	Constant Design Matrix
S	Sliding Mode Surface
D	Derivative Operator
I	Integral Operator
A	Fractional Order
$u_{Nom}^{USMC}(t)$	Nominal Control Law for Uncertain Sliding Mode Control (SMC) System
$u_{eq}^{FOUSMC}(t)$	Equivalent Control Law for Fractional Order Uncertain SMC System
K_μ	Gain of FO-ANFIS-TTS-SMC
ω_p	Neuro-Fuzzy Parameter
P	1, 2, ..., q
q	Number of Control Variables or Uncertainty Variables or Disturbance Variables
θ_p	Output of Rule Layer
$\bar{\delta}$	Uncertainty Model Output
$\bar{\omega}_p$	Ideal Value of Neuro-Fuzzy Parameter
$\Delta\omega_p$	Neuro-Fuzzy Parameter Error
ε	Unknown Parameter
τ	Design Constant
z	Special Design Variable
ρ	Adjustable Design Constant

The dynamics of precursors is modeled as:

$$\frac{dC_r(t)}{dt} = f_c((\lambda_{eff}, n_r, C_r), t) \quad (2)$$

The fuel temperature dynamics is modeled as:

$$\frac{dT_F(t)}{dt} = f_{T_F}((f_f, \mu_F, \Omega, n_r, T_F, T_C), t) \quad (3)$$

The coolant temperature dynamics is modeled as:

$$\frac{dT_C(t)}{dt} = f_{T_C}((f_f, \mu_C, \Omega, M, n_r, T_F, T_C, T_{in}), t) \quad (4)$$

The higher isotopes dynamics is modeled as:

$$\frac{dN^j(t)}{dt} = f_{N^j}((\delta_a^j; n_r, N^j, K_\infty), t) \quad (5)$$

The poisons' dynamics is modeled as:

$$\frac{dN^p(t)}{dt} = f_{N^p}((\delta_a^p; n_r, N^p, \gamma_p, \lambda_p), t) \quad (6)$$

2.2. Uncertain Two-Time Scale PWR Modeling

The PWR dynamics is uncertain due to three distinct operating conditions of reactor core. BOC, MOC and EOC are the beginning, middle and end of core fuel cycle conditions respectively. Reactor core parameters involve fast and slow dynamic modes. Fast modes are neutronic parameters such as precursors, burn-up and neutron power etc. while slow parameters are thermal parameters such as fuel temperature, and moderator / coolant temperature etc. Therefore, this is a two-time-scale problem of PWR dynamics.

The two-time-scale dynamics of PWR in state space form is given as:

$$\dot{x}_1(t) = A_{11}^j x_1(t) + A_{12}^j x_2(t) + B_1^j u(t) + B_1^j \delta(t) + B_{d_1}^j d(t) \quad (7)$$

$$\mu \dot{x}_2(t) = A_{21}^j x_1(t) + A_{22}^j x_2(t) + B_2^j u(t) + B_2^j \delta(t) + B_{d_2}^j d(t) \quad (8)$$

$$y(t) = c_1^j x_1(t) + c_2^j x_2(t) \quad (9)$$

Now, the two-time-scale dynamics of PWR can be formulated in terms of uncertain domain as:

$$M_\mu \dot{x}(t) = \sum_{j=1}^{n_h} \psi_R^j(\phi(t)) [A^j x(t) + B^j u(t) + B^j \delta(t) + B_{d_j}^j d(t)] \quad (10)$$

$$y(t) = \sum_{j=1}^{n_2} \psi_R^j(\phi(t)) c^j x(t) \quad (11)$$

2.3. Fractional Order ANFIS TTS SMC Modeling

The design framework of FO-ANFIS-TTS-SMC is shown in Figure 1. The proposed model is developed based on nonlinear singularly perturbed uncertain system dynamics, fractional calculus, sliding mode control and fractional order adaptive law.

The sliding mode surface for FO-ANFIS-TTS-SMC is basically a fractional order fuzzy sliding mode surface having constant design matrix satisfying invertible part with input matrix influenced by perturbation parameter within a finite time and robust performance and is defined as:

$$S(t) = GD^{1-\alpha} [M_\mu] - I^\alpha \left[G \sum_{j=1}^{n_2} \sum_{i=1}^{n_2} \psi_R^j(\phi(t)) \psi_R^i(\phi(t)) \cdot (A^j + B^j K_\mu^j) x(t) \right] \quad (12)$$

When states of uncertain two-time-scale system lies on the sliding mode surface $S(t)$ then it holds the following condition:

$$D^\alpha S(t) = 0 \quad (13)$$

By substituting the value of $S(t)$ from equation (12) into equation (13), we get the equivalent control law for FO uncertain SMC is given as:

$$u_{eq}^{FOUSMC}(t) = \sum_{i=1}^{n_2} \psi_R^i(\phi(t)) K_\mu^i x(t) - \delta(t) = u(t) \quad (14)$$

Now, substituting the value of $u_{eq}^{FOUSMC}(t)$ from equation (14) into equation (10), the fractional order sliding mode dynamics can be calculated as:

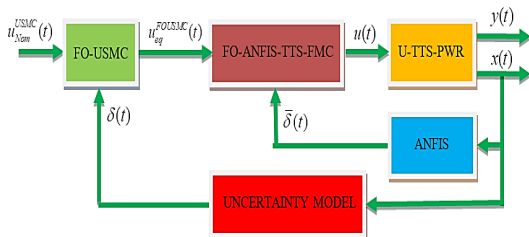


Fig. 1. Framework of FO-ANFIS-TSS-SMC for uncertain PWR dynamics.

$$M_\mu \dot{x}(t) = \sum_j \sum_{i=1}^{n_2} \psi_R^j(\phi(t)) \psi_R^i(\phi(t)) [(A^j + B^j K_\mu^j) x(t) + B_d^j d(t)] \quad (15)$$

ANFIS is used to identify the uncertainty model as:

$$\bar{\delta}(t) = \bar{\delta}_p(t) = w_p^T \theta_p(t) \quad (16)$$

The ideal neuro-fuzzy parameter is given as:

$$\tilde{w} = \tilde{w}_p = w_p - \Delta w_p \quad (17)$$

The desired control law can be deduced as:

$$u(t) = \sum_{i=1}^{n_2} \psi_R^i(\phi(t)) K_\mu^i x(t) - \tilde{w} \bar{\delta}(t) - \left(\sum_{j=1}^{n_2} \psi_R^j(\phi(t)) G B^j \right)^{-1} \cdot \frac{S(t)}{\|S(t)\|} z(t) \quad (18)$$

The $z(t)$ can be defined as:

$$z(t) = \varepsilon \left\| \sum_{i=1}^{n_2} \psi_R^i(\phi(t)) G B^i \right\| + \tau \quad (19)$$

Now, the ideal neuro-fuzzy parameter can be computed as:

$$D^\alpha \tilde{w}(t) = \rho S^T(t) \sum_{j=1}^{n_2} \psi_R^j(\phi(t)) G B^j \bar{\delta}(t) \quad (20)$$

3. RESULTS AND DISCUSSION

The closed loop functional analysis of the proposed design, performance analyses under different scenarios are discussed in the following sections.

3.1. Closed Loop Dynamic Functional Analysis of Proposed Design

The closed loop framework of reactor power transient system is shown in Figure 2. Change in reactor power will result change in neutron flux and thereby all reactivity components will change due to fissile, fertile and poison nuclides. Therefore, the reactivity due to fuel burn-up / fuel depletion dynamics will change and hence the net reactivity will change. The block diagram of closed loop framework system is shown in Figure 3. The block diagram incorporates all set-point signal, output signal, controller model, point reactor kinetics model, burn-up model, fission poison model,

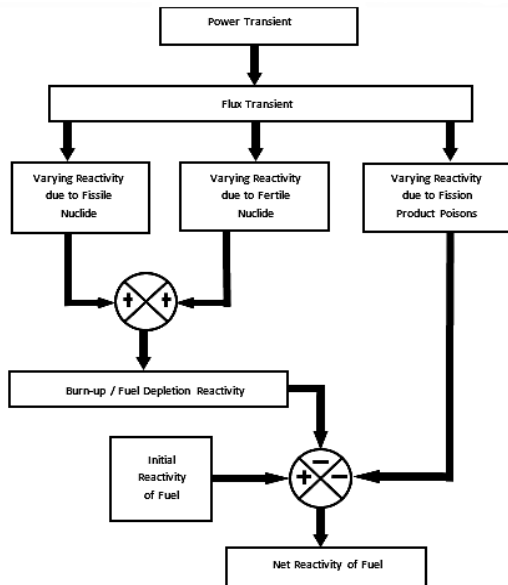


Fig. 2. Block diagram of reactor power transient framework.

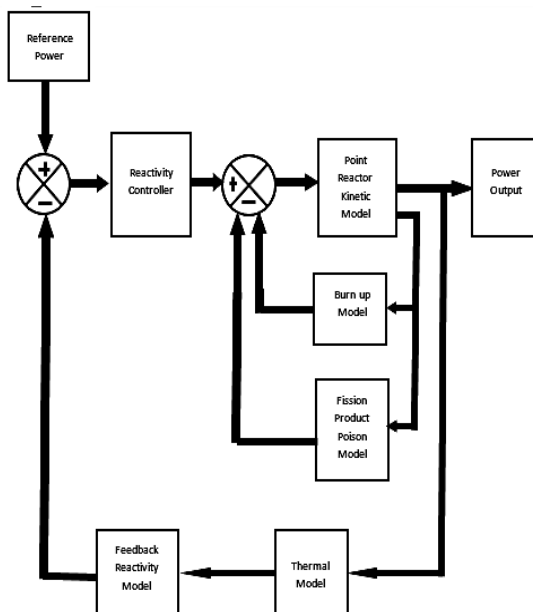


Fig. 3. Block diagram of closed loop system framework.

thermal model and reactivity model. The output of the reactivity feedback model is reactor power which is being utilized for thermal parameters.

3.2. Closed Loop Dynamic Performance Analysis of Proposed Design Under Different Scenarios

All the equations (1) through (20) are modeled in MATLAB Simulink environment and the integrated model is shown in Figure 4. The integrated simulation model is user friendly, and the operator

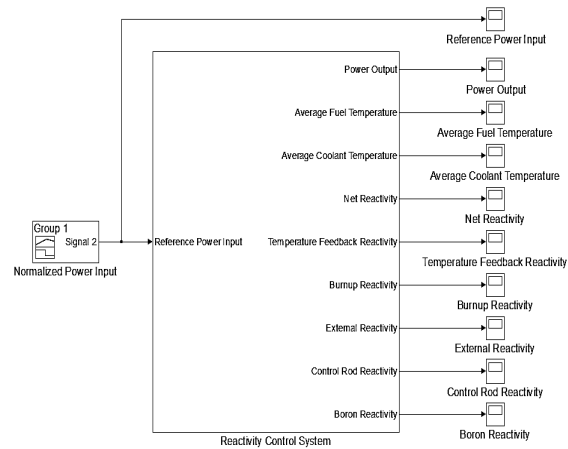


Fig. 4. Simulink closed loop model of FO-ANFIS-TTS-SMC for uncertain PWR dynamics.

/ designer / user set the desired target power and the designed parameters of interest are simulated and displayed accordingly. All model parameters shown in Figures (5-17) are basically reactivity components and are covered under reactor dynamics in terms of feedback so their dynamic behavior is deemed necessary for effectiveness of this research work in view of normal and stressed emergency operation of PWR.

This Simulink model shows a single block model of the reactivity control system considering all feedback. This model shows the input and outputs of the complete reactivity control system. Reference input power is the input to the control system while the normalized power output power, average fuel temperature, average coolant temperature, net reactivity, temperature feedback reactivity, burn-up reactivity, external reactivity, control rod reactivity and boron reactivity are the outputs.

The control design is attempted in two stages. In first stage, controller deals with external reactivity insertion or removal as control rod reactivity only. It has thermal reactivity feedback and to be analyzed and validated under normal load following operation and stressed emergency operation. In second stage, control system is multi-purpose control with additional feedback due to fuel burn-up and poisons. It incorporates reactivity control with Chemical Shim (Boron) as well as Control Rod as external reactivity controller and has capability of selection between the control mechanisms under specified conditions. It is to be

analyzed and validated under constant full power operation and partial low power operation with high and low power transient rate. Following configurable options are embedded in the proposed closed loop design:

- 1) Controller structure
- 2) Time domain (continuous or discrete)
- 3) Initial conditions and reset trigger
- 4) Output saturation limits
- 5) Signal tracking for bump-less control transfer and multi-loop control

The FO-ANFIS-TTS-SMC is the reactivity controller using Simulink environment. This controller model neither contains fuel burn-up and poison feedback reactivity nor reactivity compensation due to Boron concentration variation in the moderator. It has only thermal feedback reactivity and the control rod external reactivity. Therefore, this reactivity controller is assessed for power transients only.

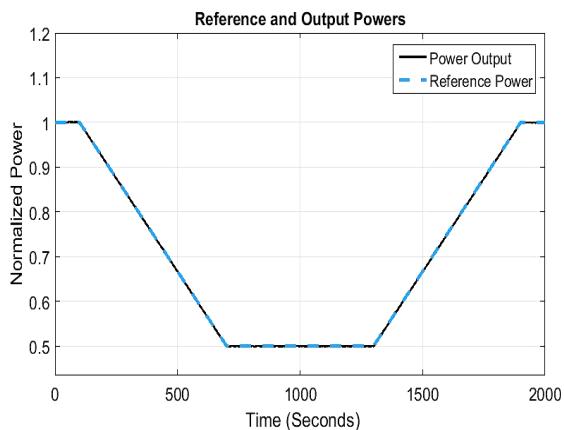


Fig. 5. Normal load following operation of PWR.

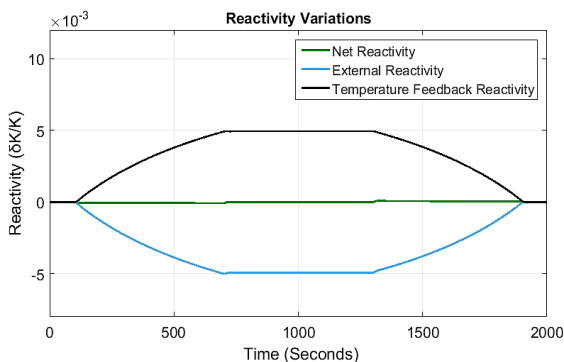


Fig. 6. Compensation of external reactivity with thermal feedback under normal load following operation in PWR.

The analysis of the reactivity controller with only thermal feedback is considered for two different scenarios. First scenario is normal load following operation while second scenario is stressed emergency operation. In normal load following operation, a load variation within 50–100% of nominal power at a ramp rate of 5% per minute is attempted.

Figure 5 shows the normal output power follows the normalized reference power input. Figure 6 shows the variation in temperature feedback reactivity, external reactivity and net reactivity for normal load following operation scenario. External reactivity follows the temperature profiles. Net reactivity has small non-zero values during power transient period.

Now, a stressed emergency operation is considered in which a load variation within from 100% to 30% of nominal power at a ramp rate of 15% per minute is attempted.

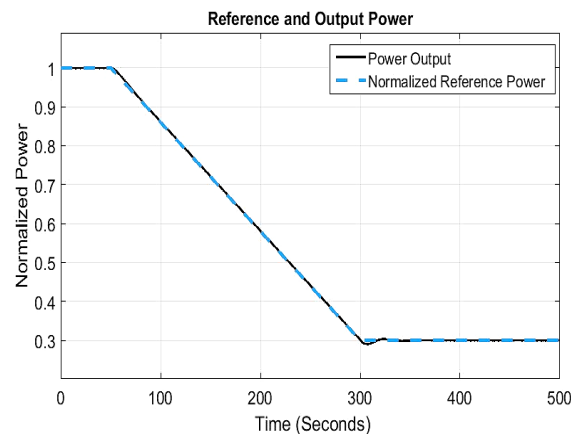


Fig. 7. Simulation of stressed emergency operation in PWR.

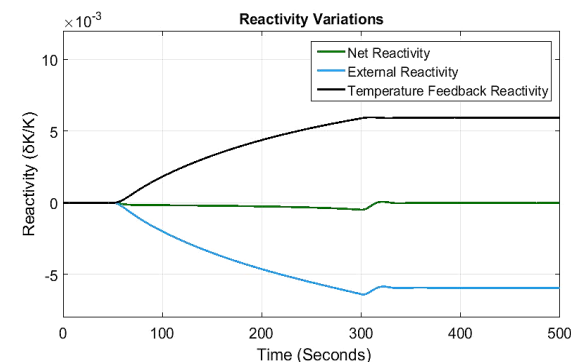


Fig. 8. Compensation of external reactivity with thermal feedback under stressed emergency operation in PWR.

Figure 9 shows the comparison of predicted boron reactivity with benchmark (FSAR). Boron reactivity model is validated by operating the reactor at constant full power for 380 days (i.e., one complete fuel cycle). Research is further extended for the reactivity controller with all feedback and both control rod reactivity and boron reactivity as external reactivity mechanisms for two different scenarios. First scenario is relatively higher power rate transient and other scenario is a lower power rate transient. During both the scenarios, reactor undergoes partial low power operation for 50 days during one complete cycle of the reactor operation.

In higher power rate transient operation, the reactor is operated at 50% power for 50 days after full power operation for 100 days. After 50 days, the reactor is again operated at full power for remaining next days of the reactor operation. The power transient rate is 10% per day. It is equivalent to 0.006944% per minute or 0.00011574% per second which is greater than lower bound i.e. 0.0000232% per

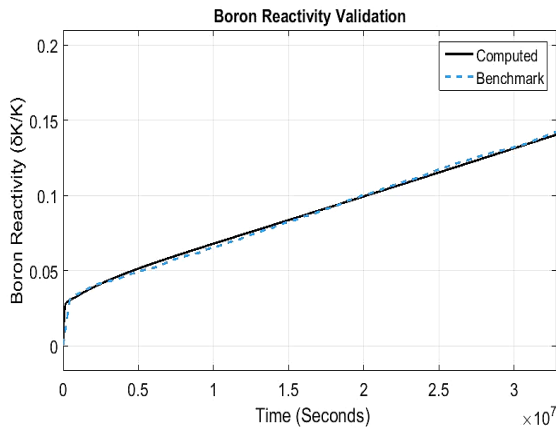


Fig. 9. Comparison of Boron reactivity with benchmark under lower rate operation in PWR.

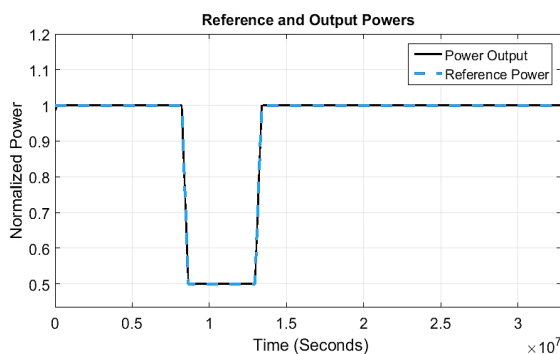


Fig. 10. Simulation of higher transient rate operation in PWR.

second. This lower bound is the minimum power transient rate for the control rod reactivity insertion or removal and below this rate only boron will control the reactivity during the slower transient. So, the control rod must react for reactivity insertion and removal during this scenario.

Figure 10 shows the normal output power follows the normalized reference power input. Figure 11 shows the variation in all internal, external and net reactivity for higher transient rate operation scenario.

It is evident from this high-power rate transient that the burn-up reactivity for higher transient rate operation has a significant variation in it due to power transient as compared to that during full power operation. The temperature reactivity feedback has a small positive value during the transient. Control rod responded as expected during transient due to higher transient rate. Boron reactivity has a little more variation during transient than that during constant full power operation. External reactivity is the sum of the boron reactivity and control rod reactivity. Net reactivity is almost zero maintaining the reactor criticality.

In lower power rate transient operation, the reactor is operated at 90 % power for 50 days after full power operation for 100 days. After 50 days the reactor is again operated at full power for remaining next days of the reactor operation. The power transient rate is 2% per day. It is equivalent to 0.001389% per minute or 0.00023148% per second which is still lower than lower bound. So, the control rod must not react for reactivity insertion and removal during this scenario.

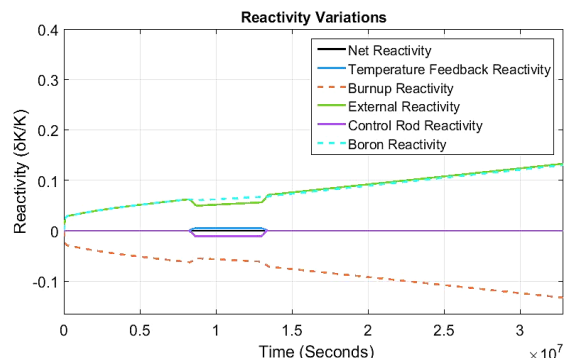


Fig. 11. Compensation of external reactivity with all feedback under higher rate operation in PWR.

Figure 12 shows the normal output power follows the normalized reference power input. Figure 13 shows the variation in all internal, external and net reactivity for lower transient rate operation scenario. It is evident from this low-power rate transient that the burn-up reactivity for lower transient rate operation has a small variation in it due to power transient as compared to that during full power operation. The temperature reactivity feedback has a small positive value during transient. Control Rod did not respond as expected during transient due to lower transient rate. Boron reactivity has a little more variation during transient than that during constant full power operation and during transient it compensates the temperature reactivity feedback because of no control action from control rod. External reactivity is the equivalent to the boron reactivity because control rod reactivity is zero. Net reactivity is almost zero maintaining the reactor criticality.

3.3. Validation of Proposed Closed Loop Design

Simulation results are validated by comparing the specific important parameters with benchmark values taken from Final Safety Analysis Report

(FSAR) of PWR [4] core for same power perturbations. Validation of results for different scenarios are discussed below. Figure 14 shows comparison of steady state values of average coolant temperature for normal load following operation scenario. The range of y-axes of Figures (14-17) is so chosen to visualize the impact of both high and low power operations on same scale. The absolute error at 100% power is 0.1655% while at 50% power is 0.856%. Figure 15 shows comparison of steady state values of temperature feedback reactivity for normal load following operation scenario. This shows that there is small difference of 10 pcm in computed temperature feedback reactivity value and benchmark temperature feedback reactivity value. It is corresponded to small absolute error of 1.98%.

Figure 16 shows comparison of steady state values of average coolant temperature for stressed emergency operation scenario. The absolute error at 100% power is 0.1655% while at 30% power is 1.9%. Figure 17 shows comparison of steady state values of temperature feedback reactivity for stressed emergency operation scenario. This shows that there is small difference of 14 pcm in

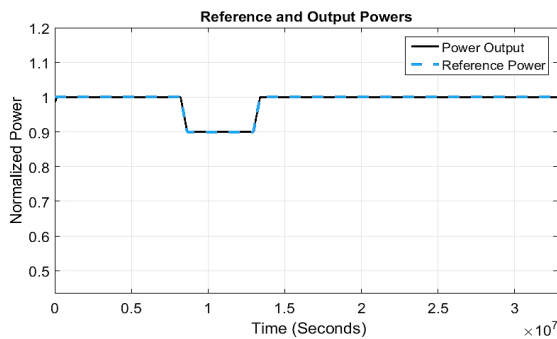


Fig. 12. Simulation of lower transient rate operation in PWR.

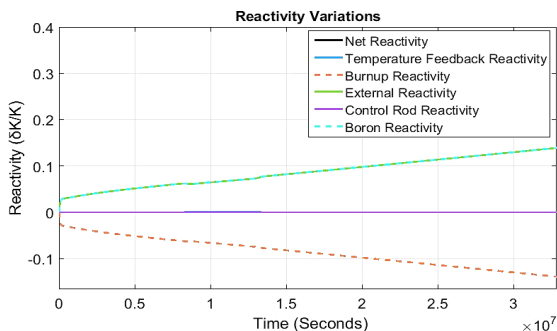


Fig. 13. Compensation of external reactivity with all Feedback under lower rate operation in PWR.

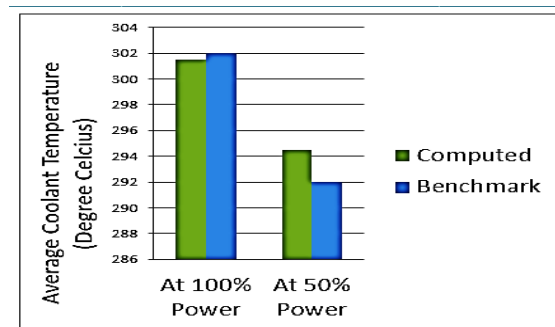


Fig. 14. Validation of average coolant temperature under normal load following operation of PWR.

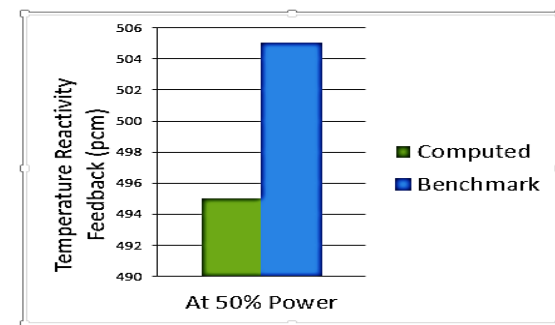


Fig. 15. Validation of thermal feedback under normal load following operation of PWR.

computed temperature feedback reactivity value and benchmark temperature feedback reactivity value. It is corresponded to a small error of 2.29%.

Figure 18 shows comparison of values of boron reactivity for constant full power operation scenario at the End of Cycle (EOC). This shows that there is a small difference of $0.003 \delta K/K$ in computed boron reactivity value and benchmark boron reactivity value. It is corresponded to an absolute error of 2.05 %. Figure 19 shows comparison of steady state values of average coolant temperature

for higher transient rate operation scenario. The absolute error at 100% power is 0.1655% while at 50% power is 0.856%. Figure 20 shows comparison of steady state values of temperature feedback reactivity for higher transient rate operation scenario. There is small difference of 10 pcm in computed temperature feedback reactivity value and benchmark temperature feedback reactivity value. It is corresponded to a small absolute error of 1.98%. Figure 21 shows comparison of steady state values of average coolant temperature for lower transient rate operation scenario. The absolute error

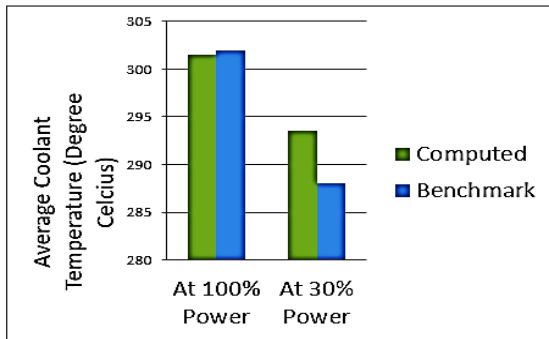


Fig. 16. Validation of average coolant temperature under stressed emergency operation of PWR.

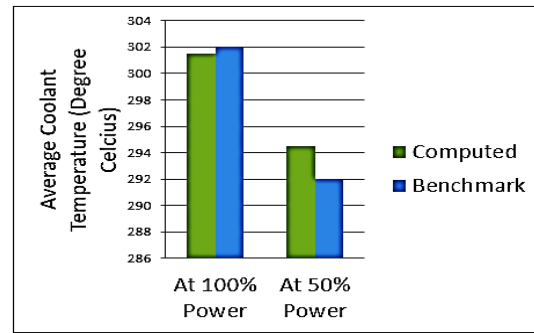


Fig. 19. Validation of average coolant temperature under high-rate operation of PWR.

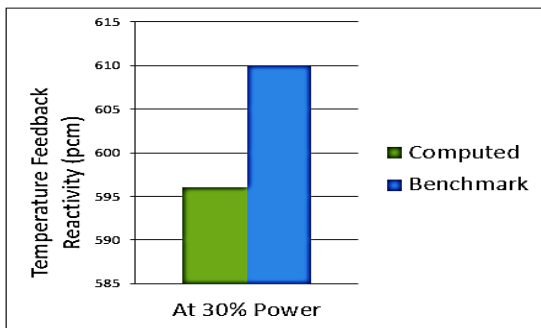


Fig. 17. Validation of thermal feedback under stressed emergency operation of PWR.

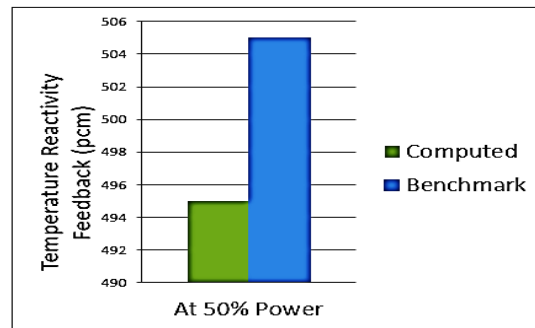


Fig. 20. Validation of thermal feedback under high-rate operation of PWR.

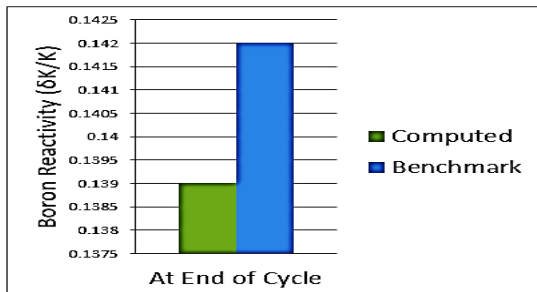


Fig. 18. Validation of Boron feedback under low-rate operation of PWR.

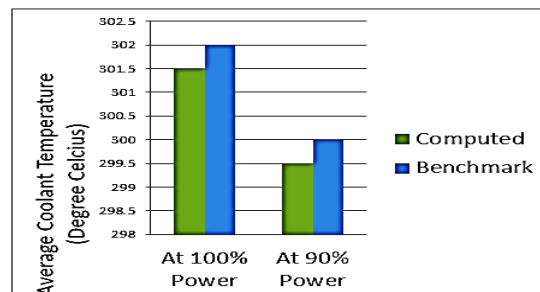


Fig. 21. Validation of average coolant temperature under low-rate operation of PWR.

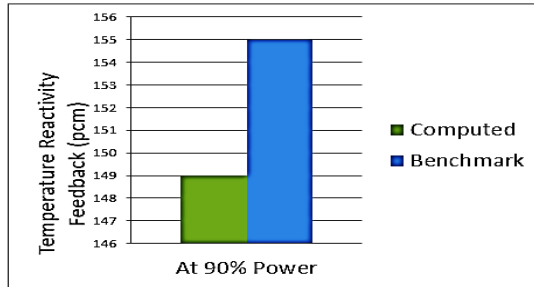


Fig. 22. Validation of thermal feedback under low-rate operation of PWR.

at 100% power is 0.1655% while at 90% power is 0.167%. Figure 22 shows comparison of steady state values of temperature feedback reactivity for lower transient rate operation scenario. This shows that there is a difference of 6 pcm in computed temperature feedback reactivity value and benchmark temperature feedback reactivity value. It is corresponded to an absolute error of 3.87%.

The desired objective of this research study is established for controlling PWR dynamics incorporating dynamic uncertainties due to fuel burn-up and thermal reactivity variation under various conditions in two-time-scale framework. The proposed scheme is proved effective by maintaining the net reactivity zero under all transient conditions. Simulation results prove that the proposed scheme is excellent in robust performance and the simulated results are most reliable as compared with benchmark results obtained from the operating PWR under the same standard conditions as mentioned in benchmark FSAR. The scope of this research work is justified after validating the results with benchmark results. The state transitions between the scales is computed and found 0.12 second. This time scale separation factor shows that dynamic behavior of reactivity components is so sharp and dynamic performance is bump less.

4. CONCLUSIONS

A lumped parameter thermo-neutronic model of PWR is developed in two-time scale framework. Fuel burn-up model is the new value addition in this research work. Fractional order ANFIS based two-time scale sliding mode external reactivity controller is designed for both control rod and boron reactivity control mechanisms and remarkable performance is observed. Simulation results prove that closed

loop dynamics is robustly stable with a desired performance. The state trajectories of proposed closed loop system converge asymptotically with disturbance rejection and excellent robust stabilization is achieved in terms of settling time and overshoot. PWR dynamics model can be extended by incorporating other primary, balance of plant and secondary systems in future.

5. ACKNOWLEDGEMENTS

The support of Sindh Institute of Management and Technology, Information Support Division of KNPGS and Mehran University of Engineering and Technology, is gratefully acknowledged.

6. CONFLICT OF INTEREST

The authors declare no conflict of interest.

7. REFERENCES

1. A.S. Reddy and G.N. Reddy. An Adaptive Fractional Order Controller Design: A Realization for Liquid Level Regulation in Liquid Level Plant. *Measurement: Sensors* 31: 100977 (2024).
2. O. Safarzadeh and O. Noori-kalkhoran. A Fractional PID Controller based on Fractional Point Kinetic Model and Particle Swarm Optimization for Power Regulation of SMART Reactor. *Nuclear Engineering and Design* 377: 111137 (2021).
3. S. Ahmed, K.K. Abulraheem, A.O. Tolokonsky, and H. Ahmed. Active Disturbance Rejection Control of Pressurized Water Reactor. *Annals of Nuclear Energy* 189: 109845 (2023).
4. S. Hussain, A.I. Bhatti, A. Samee, and H. Qaiser. Estimation of Precursor Density of a Power Using Uniform Second Order Sliding Mode Observer. *Annals of Nuclear Energy* 54: 233-239 (2013).
5. H. Asgharpour-Alamdari. Optimal Fractional Order Adaptive Neuro Fuzzy Inference System based Droop Controller for DFIG Wind Turbine to Control Load Frequency of Hybrid Microgrid. *Journal of Numerical Modelling: Electronic Networks* 35: e2942 (2021).
6. N. Ullah, S. Han, and M. Khattak. Adaptive Fuzzy Fractional Order Sliding Mode Controller for a Class of Dynamical Systems with Uncertainty. *Transactions of the Institute of Measurement and Control* 38(4): 402-413 (2016).
7. X. Liang and J. Fei. Adaptive Fractional Fuzzy Sliding Mode Control of Micro-gyroscope based

- on Backstepping Design. *Plos One* 14(6): e0218425 (2019).
8. J. Fei and C. Lu. Adaptive Fractional Order Sliding Mode Controller with Neural Estimator. *Journal of the Franklin Institute* 355(5): 2369-2391 (2018).
 9. X. Chen, W. Liang, H. Zhao, and A.A. Mamun. Adaptive Fractional Order Sliding Mode Controller with Neural Network Compensator for an Ultrasonic Motor. *ArXiv Preprint ArXiv:2103.12327* (2021).
 10. H.B. Kirgni, J. Wang, and A. Asif. Static output Feedback H_∞ based Integral Sliding Mode Control Law Design for Nuclear Reactor Power Level. *Progress in Nuclear Energy* 150: 104296 (2022).
 11. P.V. Surjagade, J. Deng, V. Vajpayee, V.M. Becerra, S.R. Shimjith, and A.J. Arul. Fractional Order Integral Sliding Mode Control of PWR Nuclear Power Plant. *European Control Conference, (12th – 15th July 2022), London, United Kingdom* (2022).
 12. D. Zhang, L. Cao, and S. Tang. Fractional Order Sliding Mode Control for a Class of Uncertain Nonlinear Systems based on LQR. *International Journal of Advanced Robotic Systems* 14(2): 1-15 (2017).
 13. A. Boubakir, F. Boudjema, and S. Labiod. A Neuro-Fuzzy Sliding Mode Controller Using Nonlinear Sliding Surface Applied to the Coupled Tanks System. *International Journal of Automation and Computing* 6: 72-80 (2009).
 14. J. George and G. Mani. A Portrayal of Sliding Mode Control through Adaptive Neuro Fuzzy Inference System with Optimization Perspective. *IEEE Access* 12: 3222-3239 (2024).
 15. K. Akbari, B. Rezaie, and S. Khari. Designing Full order Sliding Mode Controller based on ANFIS Approximator for Uncertain Nonlinear Chaotic Systems. *International Journal of Industrial Electronics, Control and Optimization* 2(1): 39-46 (2019).
 16. J. Fei and X. Liang. Adaptive Backstepping Fuzzy Neural Network Fractional Control of Micro-gyroscope using a Nonsingular Terminal Sliding Mode Controller. *Complexity* 2018: 246074 (2018).
 17. Y. Fang, F. Chen, and J. Fei. Multiple Loop Fuzzy Neural Network Fractional Order Sliding Mode Control of Micro Gyroscope. *Mathematics* 9(17): 2124 (2021).